photonics

MDPI

Communication

Cascaded Third-Harmonic Generation in Optically induced 3D Nonlinear Photonic Crystals

Tianxiang Xu [1,2], Sen Wang [1,2], Jing Zeng [1,2], Dawei Liu [3], Ruwei Zhao [1,2], Yuming Yao [1,2], Yuhao Zhao [1,2], Hui Zhao [1,2], Tiefeng Xu [1,2,4] and Yan Sheng [1,2,*]

1 Laboratory of Infrared Materials and Devices, Research Institute of Advanced Technologies, Ningbo University, Ningbo 315211, China
2 Engineering Research Center for Advanced Infrared Photoelectric Materials and Devices of Zhejiang Province, Ningbo University, Ningbo 315211, China
3 Department of Electronic Materials Engineering, Research School of Physics, Australian National University, Canberra, ACT 2601, Australia
4 Ningbo Institute of Oceanography, Ningbo 315832, China
* Correspondence: shengyan@nbu.edu.cn

Abstract: Nonlinear photonic crystals with 3D orthorhombic lattice structures were fabricated using the femtosecond laser-poling technique in ferroelectric $Sr_{0.28}Ba_{0.72}Nb_2O_6$ (SBN) crystals. The crystals were used to demonstrate the possibility of generating cascaded third-harmonic waves in optically poled ferroelectric structures. The spectral response and conversion efficiency of the third-harmonic process were experimentally investigated. While the nonlinear cascading processes can be commonly realized in electric-field-poled ferroelectric crystals, their generation in optically poled ferroelectric domain structures have not been reported elsewhere. In addition to the fully phase-matched nonlinear interaction, Cherenkov-type third-harmonic generation that fulfills the longitudinal phase-matching condition was also experimentally studied. Our study contributes to exploring the full potential of optically induced nonlinear photonic crystals and provides a new choice of materials for third-harmonic generation.

Keywords: third-harmonic generation; quasi-phase matching; 3D nonlinear photonic crystal; femtosecond laser poling

check for updates

Citation: Xu, T.; Wang, S.; Zeng, J.; Liu, D.; Zhao, R.; Yao, Y.; Zhao, Y.; Zhao, H.; Xu, T.; Sheng, Y. Cascaded Third-Harmonic Generation in Optically induced 3D Nonlinear Photonic Crystals. *Photonics* **2024**, *11*, 313. https://doi.org/10.3390/photonics11040313

Received: 23 February 2024
Revised: 25 March 2024
Accepted: 26 March 2024
Published: 28 March 2024

Copyright: © 2024 by the authors. Licensee MDPI, Basel, Switzerland. This article is an open access article distributed under the terms and conditions of the Creative Commons Attribution (CC BY) license (https://creativecommons.org/licenses/by/4.0/).

1. Introduction

The periodic poling of ferroelectric crystal has important applications in nonlinear optics, integrated photonics, and quantum optics [1–6]. This procedure can traditionally be performed using the electric field poling method, in which a periodic electric field higher than the coercive field is applied to the crystal to invert is spontaneous polarization [7]. This electric method works well for fabrications of 1D and 2D ferroelectric domain structures. However, it is almost impossible to fabricate 3D domain structures using this method because spatial modulation of electric field along the depth of a crystal is very difficult. As a solution, entirely optical processing using tightly focused femtosecond laser pulses has been proposed [8–10]. The nonlinear absorption of femtosecond pulses by the material leads to a huge temperature gradient and then a thermoelectric field that inverts ferroelectric domains in the focal volume of the laser beam [8]. An obvious advantage of this optical method is that the laser beam can be focused and scanned inside transparent ferroelectric crystals such that a 3D nonlinear photonic crystal is accessible [11–14].

Nonlinear photonic crystals with complex 3D ferroelectric domain structures have been fabricated with femtosecond laser poling to explore nonlinear optical interactions with new or improved properties [15–17]. For instance, more efficient generation of a second-harmonic vortex beam was reported with 3D spiral [18] or simplified four-grating structures [19]. Nonlinear volume holography was also experimentally demonstrated for

the generation of high-order Hermite–Gaussian [16] and bottle-shaped second-harmonic beams [20]. Moreover, it was recently proposed that 3D nonlinear photonic crystals are useful for emulating spin transport with nonlinear optics, with applications ranging from high-order skyrmions to the topological Hall effect [21,22].

The studies mentioned above were mainly conducted on a single process of second-order nonlinear interaction, and the emissions of new light are usually at the second-harmonic frequency. It is well known that nonlinear processes can be cascaded to generate various effects. For example, the cascading of second-harmonic generation ($\omega + \omega = 2\omega$) and sum frequency mixing ($2\omega + \omega = 3\omega$) offers a practical way in which to achieve third-harmonic generation (THG), which has important applications, such as in time-domain measurements of near-infrared laser pulses [23] when laser beams of a short wavelength are required. Cascaded THG requires the simultaneous fulfillment of the phase-matching conditions for second-harmonic generation (SHG) and sum frequency generation (SFG). Therefore, it involves at least two reciprocal lattice vectors (RLVs), i.e., $2k_1 + G_1 = k_2$ and $k_1 + k_2 + G_2 = k_3$, where k_1, k_2, and k_3 are wave vectors of the fundamental, second-, and third-harmonic waves, respectively, and G_1 and G_2 are RLVs provided by the nonlinear photonic crystal. The cascading processes have been widely studied in electric-field-poled ferroelectric crystals [24–30], but they have not yet been reported on for optically poled crystals. The main reason is that the efficiency of the intermediate process, namely, second-harmonic generation, is usually too low to cascade the second process in optically poled ferroelectric crystals. For one thing, the optically poled structure is usually too short to obtain very high efficiency. On the other hand, the laser-induced refractive index changes as well as structural imperfections both lead to light scattering and reflection loss that restrict efficiency [31].

In this work, we designed a 3D nonlinear photonic crystal with an orthorhombic lattice structure and fabricated it using the femtosecond laser-poling technique. We demonstrated cascaded THG in this crystal with the phase-matching conditions of SHG and SFG being fulfilled, with different orders of reciprocal lattice vectors of the orthorhombic crystal. In addition, Cherenkov-type THG satisfying the longitudinal phase-matching condition has also been studied. These results contribute to a deeper understanding of nonlinear interactions in 3D nonlinear photonic structures. They are also useful for exploring the full potentials of optically induced nonlinear photonic crystals and provide a new choice of materials for the cascading of second-order nonlinear processes.

2. Structure Design

It is known that there are 14 Bravais lattices in 3D space. Each of them provides a particular distribution of RLVs in Fourier space, and thus different QPM conditions can be generated. The orthorhombic structure has full degrees of freedom in selections of lattice constants, and the properties of this structure are relatively easy to analyze thanks to the orthorhombic relations among its primary vectors [Figure 1a]. Its three primary vectors in reciprocal space can be denoted as $\boldsymbol{G}_x$, $\boldsymbol{G}_y$, and $\boldsymbol{G}_z$, and their amplitudes should be determined according to the quasi-phase-matching (QPM) conditions for cascaded THG. In this work, our target was to achieve cascaded THG at the fundamental wavelength of 1560 nm. In order to use the largest nonlinear coefficient of the crystal, d_{33}, the fundamental beam was incident along the x axis of the crystal and polarized along the z direction. Second-harmonic generation is designed to be a collinear process, which requires the primary vector $\boldsymbol{G}_x = 0.3927\ \mu m^{-1}$ in the x direction. For the second process of SFG, the RLV can be designed to direct third-harmonic emission to any spatial direction according to the following relation: $\boldsymbol{k}_3 - \boldsymbol{k}_2 - \boldsymbol{k}_1 - \boldsymbol{G} = 0$ [Figure 1b].

The RLVs of the orthorhombic structure can be expressed as $\boldsymbol{G}_{m,n,q} = m\boldsymbol{G}_x + n\boldsymbol{G}_y + q\boldsymbol{G}_z$, where $\boldsymbol{G}_x = 2\pi/\Lambda_x$, $\boldsymbol{G}_y = 2\pi/\Lambda_y$, and $\boldsymbol{G}_z = 2\pi/\Lambda_z$ are primary vectors along the x, y, and z axes, respectively. The corresponding Fourier coefficient can be calculated according to the following equation:

$$g_{mnq} = \frac{8\pi(sin(|K|R) - |K|R\ cos(|K|R))}{|K|^3 V} \quad (1)$$

where $|K| = 2\pi\sqrt{\frac{m^2}{\Lambda_x^2} + \frac{n^2}{\Lambda_y^2} + \frac{q^2}{\Lambda_z^2}}$ and $V = \Lambda_x\Lambda_y\Lambda_z$ for the orthorhombic lattice, and R is the radius of the spherical motif [32].

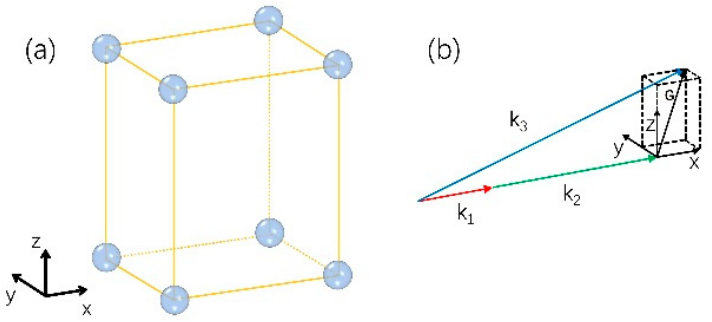

Figure 1. (**a**) The unit cell of the 3D nonlinear photonic crystal with an orthorhombic lattice structure. (**b**) The quasi-phase-matching diagram of the sum frequency generation using a noncollinear reciprocal lattice vector ***G***.

In the used $Sr_{0.28}Ba_{0.72}Nb_2O_6$ (SBN) crystal, it was found that the RLV for collinear sum frequency mixing is exactly three times that of the second-harmonic generation at the fundamental wavelength of 1560 nm. This meant that we could use $\boldsymbol{G}_x$ for SHG and $3\boldsymbol{G}_x$ for SFG. Both processes are collinear interactions, so the cascading interaction will be more efficient. If noncollinear emission of THG is required, the wave vectors of $\boldsymbol{k}_1$, $\boldsymbol{k}_2$, $\boldsymbol{k}_3$, and $\boldsymbol{G}$ need to form a close triangle, as mentioned above [Figure 1b]. Accordingly, the values of Λ_y and Λ_z can be obtained using the trigonometric functions between them.

3. Experiment

3.1. Sample Fabrication

The direct femtosecond laser-writing technique [19] was used to fabricate the nonlinear orthorhombic structures in a z-cut, as-grown SBN crystal via ferroelectric domain inversion. The SBN crystal has spontaneous ferroelectric domains of random sizes and distributions. But these random domains can only produce rather weak SHG and THG [33,34], which can be ignored when compared with the forms generated from the optically induced periodic domain patterns. A femtosecond laser source (Coherent Chameleon Ultra II) operating at 800 nm with a pulse duration of 140 fs and a repetition rate of 80 MHz was employed in the direct laser writing of ferroelectric domain patterns. The incident beam was linearly polarized along the *x*-axis of the SBN crystal. The pulse energy of the incident beam was controlled by a half-wave plate and a polarizer. In this experiment, the utilized pulse energy was about 2–4 nJ. The incident beam was focused by a 50× microscope objective with a numerical aperture (NA) of 0.65 (Olympus LCPLN50XIR). The diameter of the focused beam was about 1 μm. The SBN crystal was illuminated using the focused laser beam for 0.5 s to induce the uniform alignment of spontaneous ferroelectric domains in the focal volume of the laser pulses. After this, the laser focus was moved to the next position to repeat the ferroelectric domain inversion process, and, in this way, 3D NPCs were created.

The fabricated ferroelectric domain structures were imaged using Cherenkov second-harmonic microscopy [35–38], which works on the principle that the Cherenkov second-harmonic signal is much stronger at the ferroelectric domains that undergo an abrupt change in the second-order nonlinear coefficient. The period of the orthorhombic structure was 16(x) × 10 (y) × 25(z) μm^3, and the dimensions of the whole poled pattern were 4000(x) × 300(y) × 300(z) μm^3. A microscopic image of the fabricated structure is shown in Figure 2b.

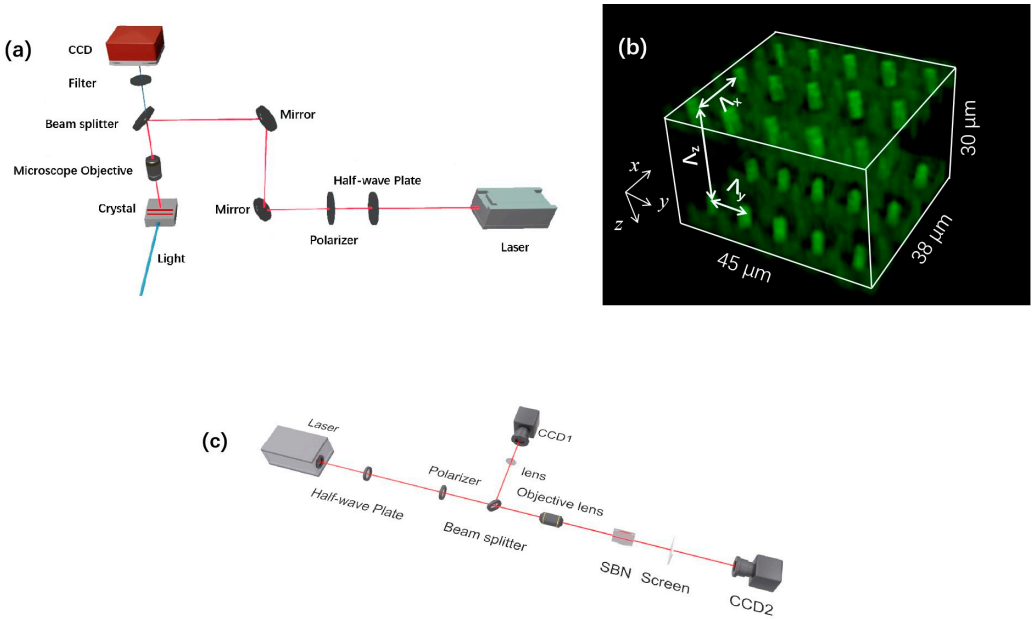

Figure 2. (**a**) The illustrative setup for optical poling of ferroelectric crystal. (**b**) The fabricated 3D nonlinear photonic crystal with orthorhombic structure, imaged using Cherenkov second-harmonic microscopy [35]. Here, the distance between the two layers of the ferroelectric domains is artificially enlarged for a better view of image. (**c**) Illustration of the setup for cascaded THG experiment.

3.2. Cascaded Third Harmonic Generation Experiment

An optical parametric oscillator (Coherent, Chameleon Compact OPO) operating at 1000–1600 nm with a pulse width of 200 fs and a repetition rate of 80 MHz was used as the fundamental beam for cascaded third-harmonic generation. This beam was linearly polarized along the *z*-axis and propagated in the fabricated NPC along the *x*-axis. The fundamental light beam was focused using a lens with a focal length of 50 mm. The beam width was estimated to be around 150 μm. The sample was mounted on the three-axis stage. The emitted second and third-harmonic waves were separately projected on a screen 1 cm away from the crystal, with appropriate filters being used to this end. The far-field harmonic profiles were recorded by a charge-coupled device (CCD) camera (HD-G230C-U3, Daheng Optics).

4. Results and Discussion

The wavelength-tuning response of the second and third harmonics was measured to find out the QPM resonances. The experimental results are shown in Figure 3a. Maximal second-harmonic generation occurred at 1550 nm, agreeing well with the intended wavelength of 1560 nm. The slight differences between the experimental and theoretic wavelengths were mainly caused by the imperfection of the fabricated nonlinear photonic structures, as random structural errors are unavoidable in any poling processes. The cascaded third-harmonic peak shifts a little bit towards the short wavelength with respect to the second-harmonic resonant wavelength, which is not surprising as cascaded THG is determined not only by the power of the intermediate second-harmonic beam but also the quasi-phase-matching conditions of the sum frequency generation process. In our experiment, the optimal quasi-phase-matching wavelengths of second-harmonic generation and sum frequency mixing occurred at different wavelengths quite often, although they were designed to occur at the same wavelength in theory. This was mainly caused by the imperfection of the fabricated structure, which is unavoidable in any poling process. In optical poling, the illumination of femtosecond laser pulses also leads to a change in the refractive index, causing the experimental perfect quasi-phase-matching wavelength to deviate from the designed wavelength too. In addition, when the second-harmonic wave becomes strong, it may revert to the fundamental wave as well. This back conversion

process competes with the sum frequency mixing, making the latter even weaker at the peak wavelength of the second harmonic. In Figure 3b,c, the recorded SH and TH images are presented to show their high quality.

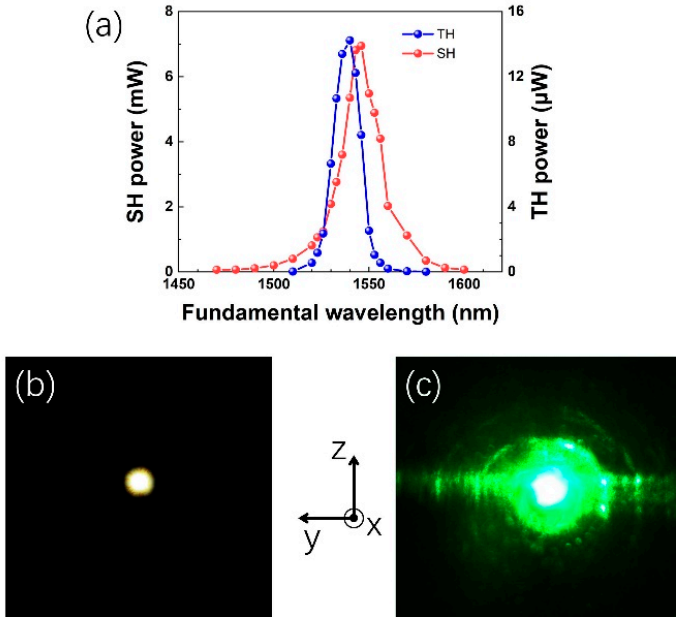

Figure 3. (**a**) The measured wavelength-tuning responses of the second- and cascaded third-harmonic generation, that is, the output power as functions of incident wavelength. (**b**,**c**) The recorded second- and third-harmonic beams in far field.

The measured dependences of the power and conversion efficiencies of the second and third harmonics on the power of the fundamental beam are presented in Figure 4. An about 4.9 mW second harmonic was obtained at a pump power of 306 mW, and the cascaded third harmonic was 13.8 μW at this pump level. The corresponding conversion efficiencies, with the Fresnel reflections from the entry and output surfaces being excluded, were 1.6% and 4.5 × 10^{-3}%, respectively. In Figure 4a, the SH efficiency keeps growing when the fundamental power is below 220 mW and presents an almost unchanged value (about 1.6%) at higher fundamental powers. The saturation of the second harmonic mainly comes from back conversion, wherein a portion of the SH wave may transform back into a fundamental wave. The results in Figure 4b show that the TH keeps growing with the pump power, so higher efficiencies can be expected if using higher pump powers beyond our experimental limits. The third-harmonic efficiency was much higher than that measured in a naturally random SBN crystal [34]. But this efficiency is still not high compared to those obtained with electric-field-poled structures. For example, the reported efficiencies were 7.5% in [24] and 12% in [39]. This is mainly because the SFM processes in this case are phase-matched using $3\boldsymbol{G}_{\mathrm{x}}$, whose Fourier coefficient is not high. It is expected that the nonlinear interaction will be much more efficient if lower-order RLVs with larger Fourier coefficients are used.

In addition to collinear THG, non-collinear emissions were observed. In Figure 5a, a cascaded third-harmonic image recorded with a longer exposure time is presented to show more detail. There are two rings that are far away from the center: these are Cherenkov third-harmonic rings [40]. Figure 5b shows a phase-matching diagram of this type of nonlinear emission. The generation of these two rings involves the RLVs $\boldsymbol{G}_{1,0,0}$ and $\boldsymbol{G}_{2,0,0}$. The experimentally measured internal emission angles are $\alpha_1 = 13.6°$ and $\alpha_2 = 9.7°$, agreeing well with the values of $\alpha_1 = 13.5°$ and $\alpha_2 = 9.4°$ calculated using the following equation: $\alpha_m = \cos^{-1}\frac{k_1+k_2+G_{m,0,0}}{k_3}$ (m = 1, 2).

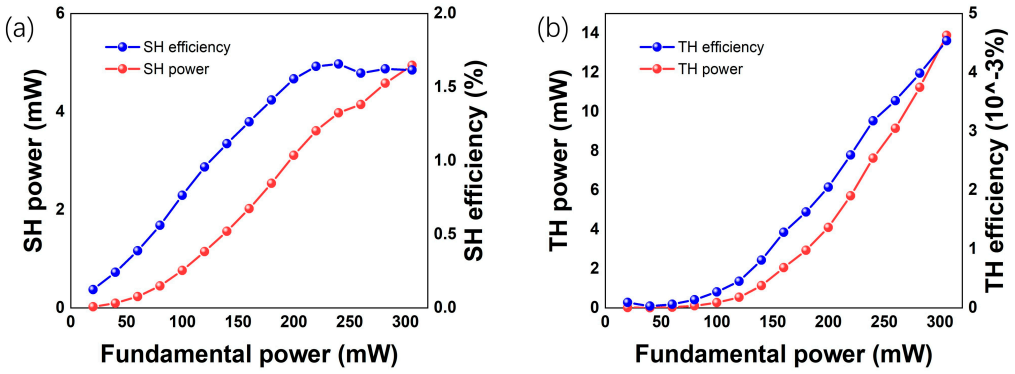

Figure 4. The measured average powers and conversion efficiencies of the second (**a**) and cascaded third harmonics (**b**) in a 3D nonlinear photonic crystal with an orthorhombic structure.

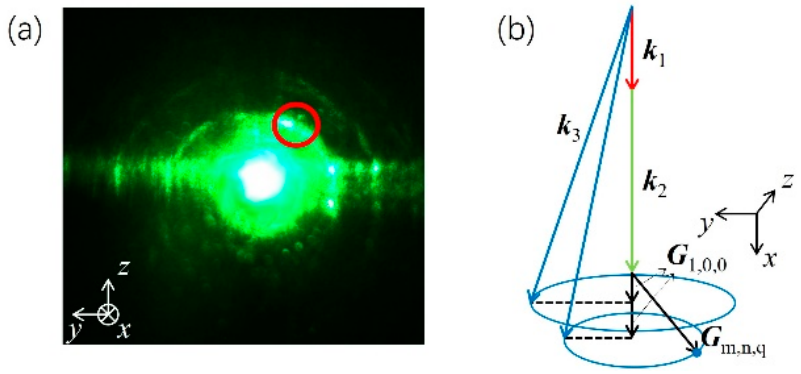

Figure 5. (**a**) An amplified view of cascaded THG taken with a longer exposure time of the CCD camera to show more detail, especially with respect to the weak TH signals. The circled bright spot is produced by $G_{2,7,5}$ (**b**) A phase-matching diagram of the Cherenkov third-harmonic generation and the RLVs that are responsible for the nonlinear Bragg diffraction.

In addition to the rings, there are also some bright third-harmonic spots scattered on the rings. They correspond to nonlinear Bragg diffraction [41], in which the full phase-matching conditions are satisfied thanks to the participation of reciprocal lattice vectors in the transverse plane. For instance, the bright spot circled in Figure 5a is produced by $G_{2,7,5}$ via nonlinear Bragg diffraction, which is also indicated by $G_{m,n,q}$ in Figure 5b. The third-harmonic image is not perfectly symmetric against its center. This might be caused by the imperfection of the poled domains structure. Meanwhile, the fundamental beam might not be perfectly normal to the crystal's surface, leading to the right side being stronger than the left. The bottom parts of the third-harmonic rings were nearly missing because they were very close to the crystal's surface and totally reflected off the crystal.

5. Conclusions

In summary, we have designed and fabricated a 3D nonlinear photonic crystal with an orthorhombic lattice structure. To this end, the femtosecond laser-poling technique was used. Cascaded third-harmonic generation was demonstrated in this crystal, with a measured efficiency of 4.5×10^{-3}% and with the phase-matching conditions of SHG and SFG being fulfilled using reciprocal lattice vectors G_x and $3G_x$, respectively. Cherenkov third-harmonic generation was also studied, with the corresponding emission angles and intensity distributions being explained in Fourier domain. Our study contributes to a deeper understanding of nonlinear interactions in 3D nonlinear photonic structures. It also provides a new choice of materials for the cascading of second-order nonlinear process.

Author Contributions: T.X. (Tianxiang Xu) and S.W., investigation and writing—review and editing; J.Z., D.L., R.Z., Y.Y., Y.Z. and H.Z., data curation; T.X. (Tiefeng Xu), funding acquisition; Y.S. writing—original draft preparation and writing—review and editing. All authors have read and agreed to the published version of the manuscript.

Funding: This work was funded by the National Natural Science Foundation of China (No. 62275136, 12274248, and 12361141815), the Natural Science Foundation of Zhejiang Province (LY22F050009), the Australian Research Council, and the K. C. Wong Magna Fund of Ningbo University.

Institutional Review Board Statement: Not applicable.

Informed Consent Statement: Not applicable.

Data Availability Statement: The data presented in this study are available on request from the corresponding author.

Conflicts of Interest: The authors declare no conflicts of interest.

References

1. Arie, A.; Voloch, N. Periodic, quasi-periodic, and random quadratic nonlinear photonic crystals. *Laser Photonics Rev.* **2010**, *4*, 355–373. [CrossRef]
2. Sun, D.; Zhang, Y.; Wang, D.; Song, W.; Liu, X.; Pang, J.; Geng, D.; Sang, Y.; Liu, H. Microstructure and domain engineering of lithium niobate crystal films for integrated photonic applications. *Light Sci. Appl.* **2020**, *9*, 197. [CrossRef]
3. Pan, J.-W.; Chen, Z.-B.; Lu, C.-Y.; Weinfurter, H.; Zeilinger, A.; Żukowski, M. Multiphoton entanglement and interferometry. *Rev. Mod. Phys.* **2012**, *84*, 777–838. [CrossRef]
4. Canalias, C.; Pasiskevicius, V. Mirrorless optical parametric oscillator. *Nat. Photonics* **2007**, *1*, 459–462. [CrossRef]
5. Ge, L.; Chen, Y.; Jiang, H.; Li, G.; Zhu, B.; Liu, Y.a.; Chen, X. Broadband quasi-phase matching in a MgO:PPLN thin film. *Photonics Res.* **2018**, *6*, 954. [CrossRef]
6. Zhang, X.; Lytle, A.L.; Popmintchev, T.; Zhou, X.; Kapteyn, H.C.; Murnane, M.M.; Cohen, O. Quasi-phase-matching and quantum-path control of high-harmonic generation using counterpropagating light. *Nature Phys.* **2007**, *3*, 270–275. [CrossRef]
7. Yamada, M.; Nada, N.; Saitoh, M.; Watanabe, K. First-order quasi-phase matched $LiNbO_3$waveguide periodically poled by applying an external field for efficient blue second-harmonic generation. *Appl. Phys. Lett.* **1993**, *62*, 435–436. [CrossRef]
8. Chen, X.; Karpinski, P.; Shvedov, V.; Koynov, K.; Wang, B.; Trull, J.; Cojocaru, C.; Krolikowski, W.; Sheng, Y. Ferroelectric domain engineering by focused infrared femtosecond pulses. *Appl. Phys. Lett.* **2015**, *107*, 141102. [CrossRef]
9. Thomas, J.; Hilbert, V.; Geiss, R.; Pertsch, T.; Tünnermann, A.; Nolte, S. Quasi phase matching in femtosecond pulse volume structured x-cut lithium niobate. *Laser Photonics Rev.* **2013**, *7*, L17–L20. [CrossRef]
10. Xu, X.; Wang, T.; Chen, P.; Zhou, C.; Ma, J.; Wei, D.; Wang, H.; Niu, B.; Fang, X.; Wu, D.; et al. Femtosecond laser writing of lithium niobate ferroelectric nanodomains. *Nature* **2022**, *609*, 496–501. [CrossRef]
11. Xu, T.; Switkowski, K.; Chen, X.; Liu, S.; Koynov, K.; Yu, H.; Zhang, H.; Wang, J.; Sheng, Y.; Krolikowski, W. Three-dimensional nonlinear photonic crystal in ferroelectric barium calcium titanate. *Nat. Photonics* **2018**, *12*, 591–595. [CrossRef]
12. Wei, D.; Wang, C.; Wang, H.; Hu, X.; Wei, D.; Fang, X.; Zhang, Y.; Wu, D.; Hu, Y.; Li, J.; et al. Experimental demonstration of a three-dimensional lithium niobate nonlinear photonic crystal. *Nat. Photonics* **2018**, *12*, 596–600. [CrossRef]
13. Imbrock, J.; Wesemann, L.; Kroesen, S.; Ayoub, M.; Denz, C. Waveguide-integrated three-dimensional quasi-phase-matching structures. *Optica* **2020**, *7*, 28–34. [CrossRef]
14. Wu, Y.; Liu, H.; Chen, X. Three-dimensional nonlinear optical holograms. *Phys. Rev. A* **2020**, *102*, 063505. [CrossRef]
15. Zhang, Y.; Sheng, Y.; Zhu, S.; Xiao, M.; Krolikowski, W. Nonlinear photonic crystals: From 2D to 3D. *Optica* **2021**, *8*, 372–381. [CrossRef]
16. Wei, D.; Wang, C.; Xu, X.; Wang, H.; Hu, Y.; Chen, P.; Li, J.; Zhu, Y.; Xin, C.; Hu, X.; et al. Efficient nonlinear beam shaping in three-dimensional lithium niobate nonlinear photonic crystals. *Nat. Commun.* **2019**, *10*, 4193. [CrossRef]
17. Chen, P.; Xu, X.; Wang, T.; Zhou, C.; Wei, D.; Ma, J.; Guo, J.; Cui, X.; Cheng, X.; Xie, C.; et al. Laser nanoprinting of 3D nonlinear holograms beyond 25000 pixels-per-inch for inter-wavelength-band information processing. *Nat. Commun.* **2023**, *14*, 5523. [CrossRef]
18. Bahabad, A.; Arie, A. Generation of Optical Vortex Beams by NonlinearWave Mixing. *Opt. Express* **2007**, *15*, 17619–17624. [CrossRef]
19. Liu, S.; Wang, L.; Mazur, L.M.; Switkowski, K.; Wang, B.; Chen, F.; Arie, A.; Krolikowski, W.; Sheng, Y. Highly Efficient 3D Nonlinear Photonic Crystals in Ferroelectrics. *Adv. Opt. Mater.* **2023**, *11*, 2300021. [CrossRef]
20. Hu, X.; Liu, S.; Xu, T.; Sheng, Y.; Zhao, R.; Krolikowski, W. Nonlinear generation of an optical bottle beam in domain-engineered ferroelectric crystals. *Opt. Lett.* **2023**, *48*, 5527–5530. [CrossRef]
21. Karnieli, A.; Tsesses, S.; Bartal, G.; Arie, A. Emulating spin transport with nonlinear optics, from high-order skyrmions to the topological Hall effect. *Nat. Commun.* **2021**, *12*, 1092. [CrossRef]

22. Yesharim, O.; Pearl, S.; Foley-Comer, J.; Juwiler, I.; Arie, A. Direct generation of spatially entangled qudits using quantum nonlinear optical holography. *Sci. Adv.* **2023**, *9*, 7968. [CrossRef]
23. Monat, C.; Grillet, C.; Collins, M.; Clark, A.; Schroeder, J.; Xiong, C.; Li, J.; O'Faolain, L.; Krauss, T.F.; Eggleton, B.J.; et al. Integrated optical auto-correlator based on third-harmonic generation in a silicon photonic crystal waveguide. *Nat. Commun.* **2014**, *5*, 3246. [CrossRef]
24. Zhu, S.; Zhu, Y.; Ming, N.b. Quasi-Phase-Matched Third-Harmonic Generation in a Quasi-Periodic Optical Superlattice. *Science* **1997**, *278*, 843–846. [CrossRef]
25. Mateos, L.; Molina, P.; Galisteo, J.; López, C.; Bausá, L.E.; Ramírez, M.O. Simultaneous generation of second to fifth harmonic conical beams in a two dimensional nonlinear photonic crystal. *Opt. Express* **2012**, *20*, 29940–29948. [CrossRef]
26. Chen, B.Q.; Zhang, C.; Hu, C.Y.; Liu, R.J.; Li, Z.Y. High-Efficiency Broadband High-Harmonic Generation from a Single Quasi-Phase-Matching Nonlinear Crystal. *Phys. Rev. Lett.* **2015**, *115*, 083902. [CrossRef]
27. Wei, D.; Guo, J.; Fang, X.; Wei, D.; Ni, R.; Chen, P.; Hu, X.; Zhang, Y.; Hu, W.; Lu, Y.Q.; et al. Multiple generations of high-order orbital angular momentum modes through cascaded third-harmonic generation in a 2D nonlinear photonic crystal. *Opt. Express* **2017**, *25*, 11556–11563. [CrossRef]
28. Chen, C.; Lu, J.; Liu, Y.; Hu, X.; Zhao, L.; Zhang, Y.; Zhao, G.; Yuan, Y.; Zhu, S. Cerenkov third-harmonic generation via cascaded χ^2 processes in a periodic-poled LiTaO3 waveguide. *Opt. Lett.* **2011**, *36*, 1227–1229. [CrossRef]
29. Fang, X.; Wei, D.; Wang, Y.; Wang, H.; Zhang, Y.; Hu, X.; Zhu, S.; Xiao, M. Conical third-harmonic generation in a hexagonally poled LiTaO3 crystal. *Appl. Phys. Lett.* **2017**, *110*, 4978669. [CrossRef]
30. Vernay, A.; Bonnet-Gamard, L.; Boutou, V.; Trajtenberg-Mills, S.; Arie, A.; Boulanger, B. High efficiency cascaded third-harmonic generation in a quasi-periodically poled $KTiOPO_4$ crystal. *OSA Continuum* **2020**, *3*, osac.395084. [CrossRef]
31. Keren-Zur, S.; Ellenbogen, T. A new dimension for nonlinear photonic crystals. *Nature Photonics* **2018**, *12*, 575–577. [CrossRef]
32. Pogosian, T.; Lai, N.D. Theoretical investigation of three-dimensional quasi-phase-matching photonic structures. *Phys. Rev. A* **2016**, *94*, 063821. [CrossRef]
33. Ayoub, M.; Roedig, P.; Imbrock, J.; Denz, C. Cascaded Čerenkov third-harmonic generation in random quadratic media. *Appl. Phys. Lett.* **2011**, *99*, 3670322. [CrossRef]
34. Wang, W.; Roppo, V.; Kalinowski, K.; Kong, Y.; Neshev, D.N.; Cojocaru, C.; Trull, J.; Vilaseca, R.; Staliunas, K.; Krolikowski, W.; et al. Third-harmonic generation via broadband cascading in disordered quadratic nonlinear media. *Opt. Express* **2009**, *17*, 20117–20123. [CrossRef] [PubMed]
35. Sheng, Y.; Best, A.; Butt, H.-J.; Krolikowski, W.; Arie, A.; Koynov, K. Three-dimensional ferroelectric domain visualization by Čerenkov-type second harmonic generation. *Opt. Express* **2010**, *18*, 16539–16545. [CrossRef] [PubMed]
36. Deng, X.; Chen, X. Domain wall characterization in ferroelectrics by using localized nonlinearities. *Opt. Express* **2010**, *18*, 15597–15602. [CrossRef] [PubMed]
37. Ayoub, M.; Futterlieb, H.; Imbrock, J.; Denz, C. 3D Imaging of Ferroelectric Kinetics during Electrically Driven Switching. *Adv. Mater.* **2017**, *29*, 3325. [CrossRef] [PubMed]
38. Kämpfe, T.; Reichenbach, P.; Schröder, M.; Haußmann, A.; Eng, L.M.; Woike, T.; Soergel, E. Optical three-dimensional profiling of charged domain walls in ferroelectrics by Cherenkov second-harmonic generation. *Phys. Rev. B* **2014**, *89*, 035314. [CrossRef]
39. Yan Sheng, S.M.S.; Kaloian, K. Cascaded third-harmonic generation in a single short-range-ordered nonlinear photonic crystal. *Opt. Lett.* **2009**, *34*, 656–658. [CrossRef]
40. Zhang, Y.; Gao, Z.D.; Qi, Z.; Zhu, S.N.; Ming, N.B. Nonlinear Cerenkov radiation in nonlinear photonic crystal waveguides. *Phys. Rev. Lett.* **2008**, *100*, 163904. [CrossRef]
41. Saltiel, S.M.; Neshev, D.N.; Fischer, R.; Krolikowski, W.; Arie, A.; Kivshar, Y.S. Generation of second-harmonic conical waves via nonlinear bragg diffraction. *Phys. Rev. Lett.* **2008**, *100*, 103902. [CrossRef]

Disclaimer/Publisher's Note: The statements, opinions and data contained in all publications are solely those of the individual author(s) and contributor(s) and not of MDPI and/or the editor(s). MDPI and/or the editor(s) disclaim responsibility for any injury to people or property resulting from any ideas, methods, instructions or products referred to in the content.